D10488

ADVMEW
ISSN 0935-9648
Vol. 18, No. 1
January 5, 2006

ADVANCED MATERIALS

WILEY-VCH

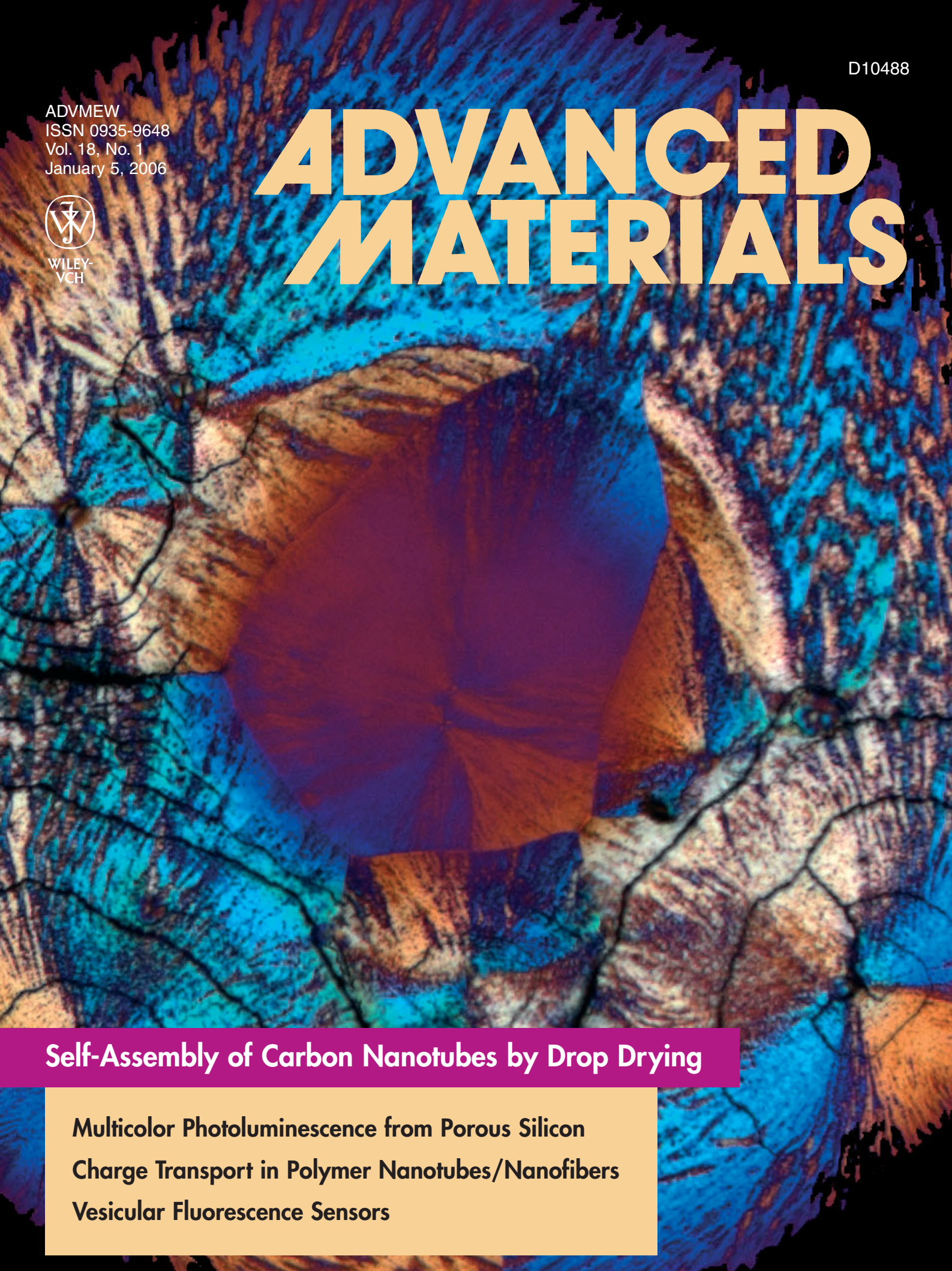

Self-Assembly of Carbon Nanotubes by Drop Drying

Multicolor Photoluminescence from Porous Silicon

Charge Transport in Polymer Nanotubes/Nanofibers

Vesicular Fluorescence Sensors

DOI: 10.1002/adma.200500625

Self-Assembly of Single-Walled Carbon Nanotubes into a Sheet by Drop Drying**

By *Rajat Duggal*, *Fazle Hussain*, and *Matteo Pasquali**

Single-walled carbon nanotubes (SWNTs) are currently the focus of extensive interdisciplinary studies because of their unique physical and chemical properties and potential electronic applications, for example, in making sensors and field-emission devices.[1] Processing of SWNT-based materials into engineered macroscopic materials is still in its infancy; the most successful methods so far have been based on adapting techniques that had been developed in other areas of material science such as colloids and polymers. Recent successes include preparing fibers and ribbons of SWNTs;[2] films of pure SWNTs,[3,4] polymers doped with SWNTs,[5,6] and growth in situ of SWNT arrays.[7] Evaporation of drops on substrates has been used for patterned deposition of solutes onto non-porous substrates, such as in DNA microarrays,[8] nanolithography,[9] protein crystallization,[10] and stretching DNA for hybridization studies.[11,12] Shimoda et al.[13] prepared continuous self-assembled films of SWNT bundles on glass near a receding contact line by solvent evaporation. The moving contact line of a drying drop could be similarly used to form aligned patterns of SWNTs on substrates for making films or for nanofabrication.

Drops of a solution on a substrate follow one of two drying mechanisms: either the drop maintains a constant contact angle by de-pinning the contact line (e.g., water on non-wetting substrates[14]), or the contact line gets pinned and the drop maintains a fixed contact area (e.g., colloidal dispersions[15]). Deegan and co-workers[15–17] have studied the drying of drops of colloidal dispersions and found that the particles deposit in a ring at the periphery of the drop due to capillary flow in which the pinned contact line causes the solvent to flow towards the edge. Recent investigations have also shown the formation of a skin or crust at the free surface of drops of polymers and colloidal suspensions.[18,19] Pauchard and Allain[19] found that the crust may collapse and evolve into different shapes as the surface area remains constant while the drop volume decreases due to solvent evaporation. "Crusting" on the surface of spin-cast films[20,21] is a well-known phenomenon. De Gennes[22] suggested a transport model for crust formation in spin-cast films. Because the glass-transition or gelation temperature of a pure polymer/colloid is higher than that in solution,[19] at any temperature below the glass transition there is a critical particle concentration at which the system transitions from fluid to glassy or gel-like. Evaporation of solvent from the free surface leads to a local increase in concentration of the polymer/suspension at the free surface, and a very thin glassy or gelled crust is formed at the free surface. Here, we investigated drying of a sessile drop of individually suspended SWNTs in an aqueous solution of F68 Pluronic. We found that, instead of assembling on the substrate, the SWNTs self-assemble into a crust at the free surface. This entangled mesh-like crust was characterized by various microscopy techniques. The "crusting" phenomenon could be used as a potential route for making thin coatings and films of SWNTs.

Video microscopy showed that the initial drying progressed by de-pinning of the contact line, i.e., the radius of the base decreased with time. Figure 1a shows the drop radius (normalized by the initial radius) as a function of time. The diameter of each drop was measured at four different angles and then averaged. After about 360 s the drop attained a fixed base radius and a foot started appearing. Drops of pure water on the same substrate dried by maintaining a fixed base radius, in agreement with the findings by Birdi et al.[23] Assuming quasistationary conditions, if diffusion of water in air is rate controlling, then in a sessile drop receding with a constant contact angle the square of the base radius is linear with time.[24] While the drop radius shrunk, the contact angle between the drop and the glass substrate was about 10–15 °C (inferred by video microscopy). Up to $t \sim 210$ s, we find that the assumption that diffusion is rate controlling is fairly accurate (Fig. 1b). We recorded the variation of weight of the drop with time (Fig. 1c) and found that the initial evaporation rate J_0 was $J_0 \sim 2 \times 10^{-6}$ cm^3 s^{-1}. As the drying progressed further, the drop attained a constant base radius at $t \sim 360$ s, and a surface undulation appeared at the top of the drop. A thin crust appeared at the free surface, with a convective flow toward the foot underneath. The formation of the crust slowed down the solvent loss from the initial evaporation rate J_0 (Fig. 1c) by reducing the diffusion of water from the core of the drop to the free surface. Loss of the solvent decreased the volume enclosed by the thin crust, and the crust thus inverted, forming an undulation similar to a collapsing dome. The drying process is summarized schematically in Figure 2.

[*] Prof. M. Pasquali, Dr. R. Duggal
Department of Chemical and Biomolecular Engineering and
Center for Nanoscale Science and Technology and
Center for Biological and Environmental Nanotechnology
Rice University
MS362, 6100 Main St., Houston, TX 77005 (USA)
E-mail: mp@rice.edu
Prof. F. Hussain
Department of Mechanical Engineering
University of Houston
Houston, TX 77204 (USA)

[**] The authors thank P. E. Laibinis, C. A. Miller, R. Sharma, M. S. Wong, C. D. Armeniades, J. M. Tour, J. Stephenson, S. Agarwal, and W. V. Knowles. We also thank R. E. Smalley and R. H. Hauge for providing the SWNT samples. We thank especially E. A. Whitsitt for SEM images, N. G. Parra-Vasquez for preparing the SWNT sample, and V. A. Davis for Raman microscopy and helpful discussions. This work was supported by the National Science Foundation through grant CTS-CAREER 0134389 and by the NSF Center for Biological and Environmental Nanotechnology (EEC-0118007). Supporting Information is available online from Wiley InterScience or from the author.

ADVANCED MATERIALS

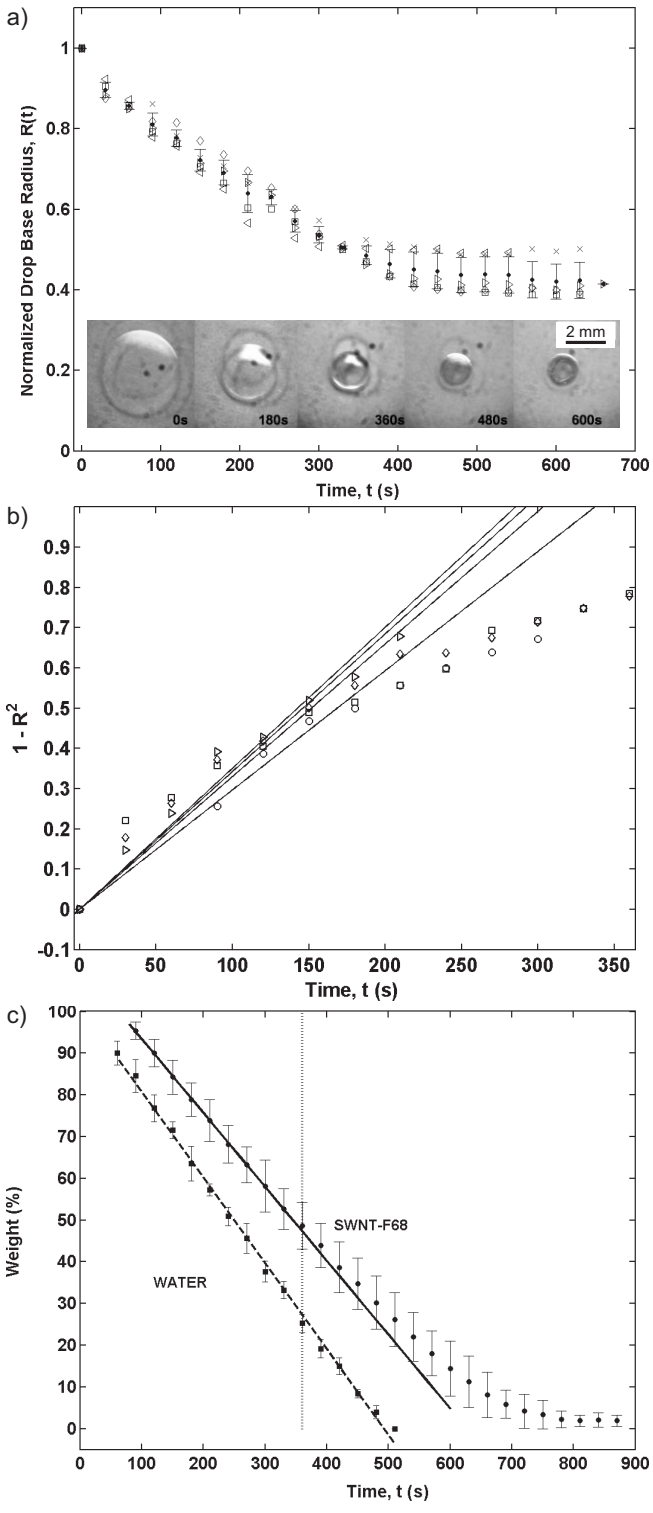

Figure 1. a) Normalized drop radius R versus time t, for five SWNT–F68 drops (1 μL) deposited on glass. After ~360 s the drops attain a fixed base radius. Time-lapse video microscopy images are also shown. b) $1-R^2$ versus time for four drops for $t<240$ s. c) Variation of drop weight versus time for SWNT–F68 (●) and water (■). Water drops dry with a constant drying rate (broken line). SWNT–F68 drops dry at a constant drying rate for $t<360$ s (solid line). For $t>360$ s the evaporation rate slows down. Averages are for 5 sets of 16 drops (SWNT–F68) and 3 sets of 16 drops (water). The error bars are the standard deviations.

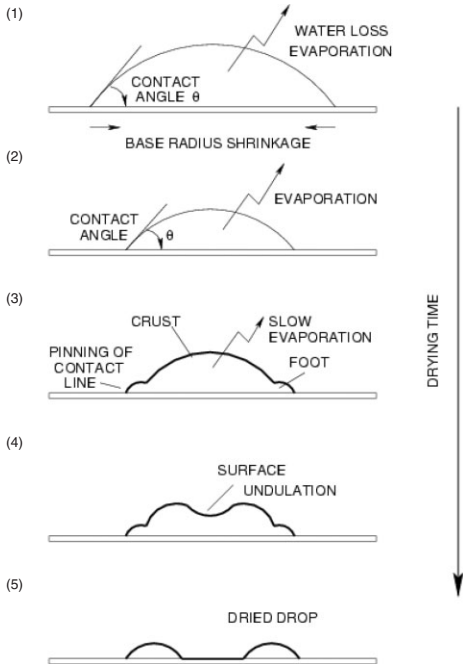

Figure 2. Schematic of the drying process. 1,2) The drop maintains a fixed contact angle as the base radius shrinks. 3) The contact line is pinned and a gelled foot appears. A crust is formed at the free surface, reducing the evaporation rate. 4) The volume that the crust envelops decreases as evaporation proceeds, and a surface undulation appears. 5) The crust sits on the surfactant-SWNT deposit on the substrate as the drying reaches completion.

In contrast to the drying drops of SWNT–F68 suspension, when aqueous drops of a SWNT-SDS suspension were dried under similar conditions, a crust did not form and the SWNTs deposited in the center of the drop. Both SDS and F68 are surface-adsorbing molecules which arrange at the free surface with the hydrophobic part at the air/water interface and the hydrophilic part suspended in water. The hydrophobic poly(propylene oxide) (PPO) chain in Pluronic surfactant arranges itself at the air/water interface, and the hydrophilic poly(ethylene oxide) (PEO) chains extend as brushes in the water.[25] Sodium dodecylsulfate (SDS)—a small molecule—cannot form a mesh to support the SWNTs, while F68—a long-chain polymer—can form an entangled network entrapping the SWNTs. Evaporative loss of the solvent, advection-driven transport of SWNT–F68, and preferential adsorption of the surfactant at the air/liquid interface lead to a local increase in the concentration of the SWNT–F68 complex at the free surface, leading to the formation of a crust.

The inhomogeneities (due to SWNTs) in the thin crust served as nucleation points for fractures. "Volcanic landscapes" appeared when the crust ruptured at isolated points (Fig. 3a (panel 2), Fig. 3b). Aligned liquid-crystalline domains (observed under polarization, Fig. 3a (panels 3–6), Fig. 3c) were formed as the evaporation front moved across the drop from the rupture sites. Defect planes appeared over time when two evaporation fronts met, akin to the formation of

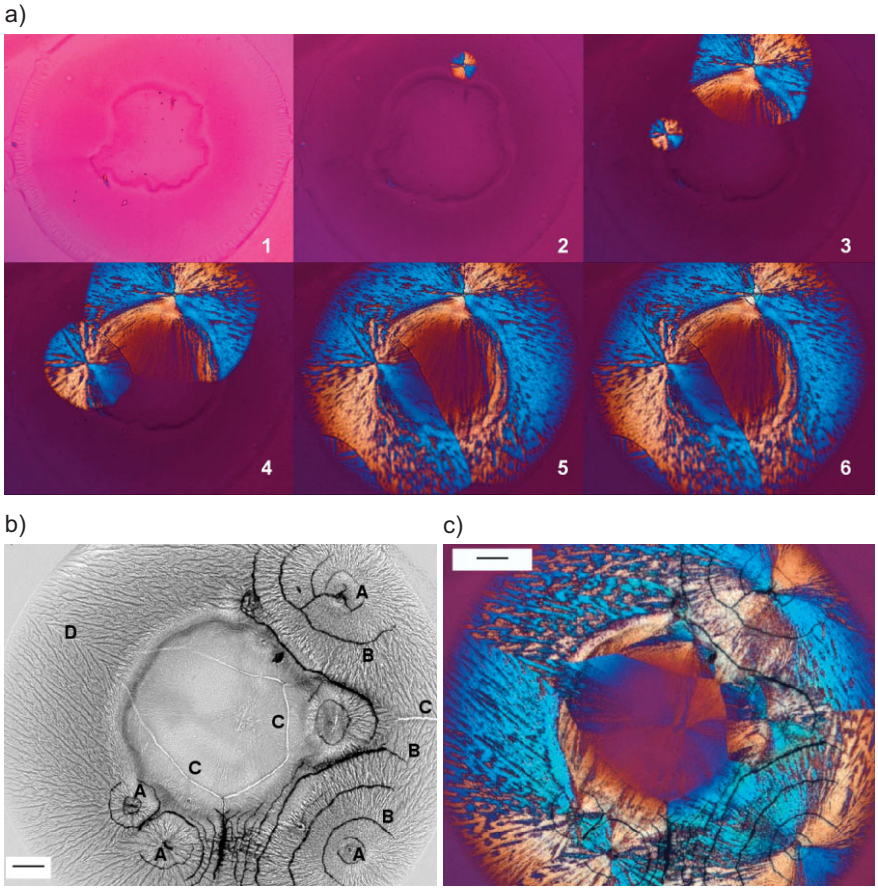

Figure 3. Dried drops of SWNT–F68 on glass. a) Progression of drying under crossed polarizers. 1) Contact line is pinned and the drop forms a gelled foot. Note the undulation of the free surface in the middle. 2) Crust ruptures at a point and birefringent patterns start appearing. 3) Crust ruptures at another point and the drying fronts move radially. 4) The drying fronts meet to form a grain boundary. 5) The drying fronts move across the whole drop. 6) A circular crack appears around the rupture site (at the top). b) Bright-field image showing the foot of the drop, volcanic landscape, and cracks. A) Rupture sites, B) cracks, C) grain boundaries, D) foot. Scale bar is 100 μm. c) Under crossed polarizers. The birefringent fan-like arrangements of the micelles, characteristic of hexagonal liquid-crystalline domains. Scale bar is 100 μm.

grain boundaries and defects in crystals (Fig. 3a (panel 4)). Further water loss occurred with the horizontal dimensions remaining fixed, and the extremely thin crust came under increasing tension (as it tried to shrink) and then fractured, forming cracks (Fig. 3a (panel 6)). The direction of the cracks at the surface may depend on the packing of the SWNT–F68 micelles. Islam et al.[26,27] recently reported similar surface cracking in dried samples of SWNTs stabilized by sodium dodecyl benzene sulfonate and trapped in nematic aqueous gels of crosslinked *N*-isopropylacrylamide. They conclude that cracking occurs because of generation of high internal stress at the surface that originates from coupling of the nematic director (packing direction) and the elasticity of the SWNT-surfactant network. The fan-like arrangement (Fig. 3c) observed (which occurred even if the SWNTs were not present, though only in the foot of the drop) is typical of hexagonal liquid-crystalline order where the solute is cylindrical in shape.[28] F68 forms only cubic liquid-crystalline phases[29] and thus should have no birefringence. Eiser et al.[30] have reported strain-induced orientation transitions in the lyotropic cubic crystalline phase of F68. Here, the convective flow in the drop aligned the micelles into columns, yielding a hexagonal arrangement. Drying drops of F68 alone did not develop a surface undulation, but a gelled foot appeared at the contact line, and a crust was formed. Structures similar to those on glass were formed on mica; Figure 4a shows an atomic force microscopy (AFM) image of aligned SWNT–F68 micelles near the edge of the drop. The striations (also seen in Fig. 3b, the spokes originate from the rupture sites (A)) are the assembled surfactant micelles. The presence of SWNTs on the surface of the dried drop was found by imaging at the cracks by scanning electron microscopy (SEM). The long rod-like structures are the SWNT–F68 micelles and not the Pluronic micelles (Fig. 4c). Such structures are particularly prominent in cracks which they bridge.

In order to investigate the structure and arrangement of the SWNT–F68 micelles in the crust, we first suspended the crust in water and floated it on aluminum SEM posts to obtain SEM images. The crust looked like a mat of entangled strands. Monolayer thin regions of the crust where the mesh was

ADVANCED MATERIALS

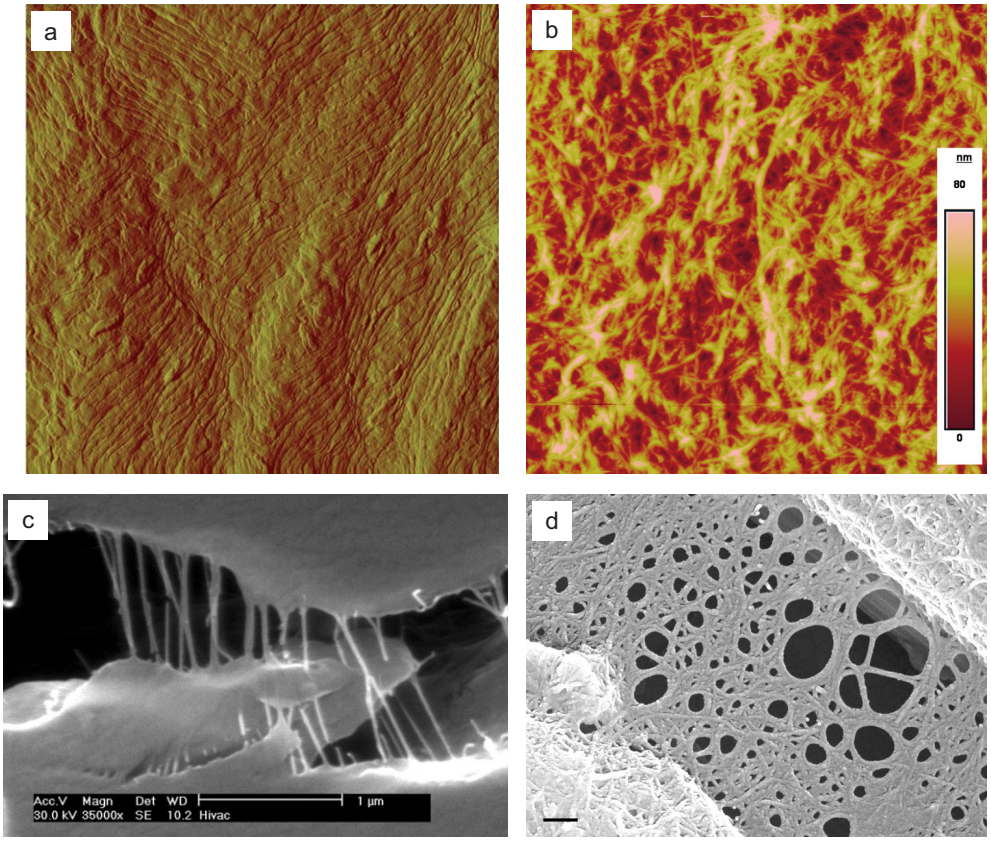

Figure 4. a) AFM amplitude scan (10 µm × 10 µm) at the surface of a dried drop of SWNT–F68 on mica. Scans were done near the edge of the drop. The striations due to the assembled polymer micelles can be seen. b) AFM scan (5 µm × 5 µm) of the crust on mica showing entangled mesh-like morphology. The height scale is 80 nm. c) SEM image showing SWNT–F68 bundled bridging a crack. d) SEM image of SWNT–F68 crust formed on glass. Note that the crust is under tension in the crack. Scale bar is 200 nm. The SEM samples (c,d) were coated with gold.

under tension (Fig. 4d) were observed. Such regions of high internal stress that lead to cracks have been not been reported before. The thickness of the crust was between 10 and 100 nm. We measured a strand size of ~10–15 nm. High-pressure CO conversion (HiPco) SWNTs have a diameter of ~1 nm,[31] and F68-coated individual SWNTs in solution have an estimated diameter of ~13 nm (using de Gennes' polymer-brush theory:[32] $L_0 = a^{5/3} N A^{-1/3}$, where L_0 is the brush length in the solvent, $N = 78$ is the number of ethylene oxide monomers, $a = 0.24$ nm is the size of the ethylene oxide monomer, and $A = 1.8$ nm^2 is the area occupied by each molecule of F68 at the air/water interface). In the absence of water, the brushes would collapse and the size of the strand around an individual SWNT would be about 5 nm. Figure 4b shows an AFM scan of the mesh-like structure of the crust. The film thickness could not be measured accurately by AFM due to folding of the crust during transfer onto mica. The crust was a monolayer thick (~10 nm) at the edges; toward the middle the surface roughness was 50–80 nm. The presence of SWNTs in the thin crust was apparent from the dark color (Fig. 5a, inset). Raman spectra of the crust showed the characteristic transverse breathing mode of SWNTs at ~1592 cm^{-1} and the radial breathing mode at ~234 cm^{-1}. The low intensity of the peaks at ~270 cm^{-1} indicated the low degree of bundling of SWNTs in the strands of the crust. To confirm the presence of SWNTs in the strands of the crust, transmission electron microscopy (TEM) was also performed on the crust floated onto non-coated copper grids. Images of the mat were obtained and SWNTs were imaged in the entangled strands (Fig. 5b). The SWNTs appeared bundled (~10 SWNTs in each bundle), but the bundles were thinner compared to those found in conventional Buckypaper. The low degree of bundling is attributed to the surfactant-SWNT dispersion that had most of the SWNTs present as individuals and the spontaneous self-assembly of individual SWNT–F68 micelles at the free surface. The low degree of bundling of SWNTs in the strands of the thin crust can be potentially beneficial in preparing thin (~100 nm) optically transparent conductive films and coatings. The electrical conductivity of the crust could not be measured accurately because the sample could not be easily mounted on the probes (to measure conductivity) due to the small dimensions (1 mm diameter) and the brittle nature of the crust. Conductive films and coatings may require baking the crust to remove the polymeric surfactant or an increased loading of SWNTs in the SWNT-polymer mixture in order to improve contacts between the nanotubes.

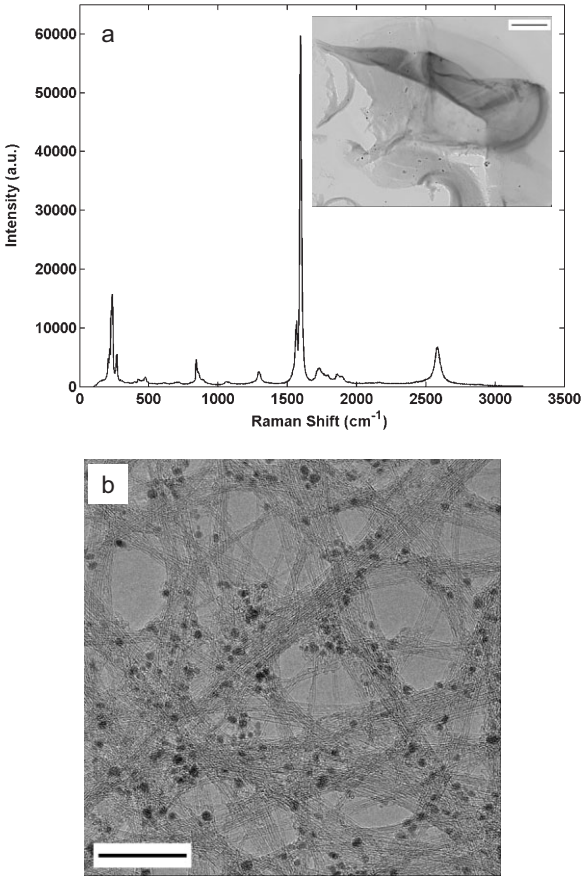

Figure 5. a) Raman spectrum of the crust displaced from a drying drop of SWNT–F68 on glass (780 nm diode laser). The peaks at ~1592 cm^{-1} and ~234 cm^{-1} correspond to the axial and radial breathing modes of SWNTs, respectively. Inset: A displaced crust. Scale bar is 200 μm. b) Transmission electron micrograph of the crust, showing the presence of SWNTs in the strands. Scale bar is 40 nm.

The simple de Gennes theory that describes formation of a crust in spin-cast films[22] is based on two assumptions: the polymer has a glass transition and the polymer is non-surface adsorbing. F68 Pluronic is a semicrystalline polymer that has a melting point of 57.2 °C (found by differential scanning calorimetry (DSC)) and no glass transition above room temperature. It is well known that addition of SWNTs to polymers can alter the glass-transition temperature. We performed DSC on dried samples of the aqueous solution and found that the presence of SWNTs did not alter the melting point of the mixture. Moreover, F68 is a surface-adsorbing polymer; thus, the de Gennes theory cannot be used to explain the SWNT–F68 system. However, the de Gennes theory can be qualitatively applied to the SWNT–F68–water system; i.e., an entangled mesh is formed at the free surface because, first, the mixture transitions from liquid-like to solid-like at the free surface due to loss of solvent, and second, the preferential adsorption of part of the surfactant (F68) at the air/water interface leads to the transport of nanotubes to the surface. To find the critical concentration of the polymer required at the free surface to form a crust, we measured the linear viscoelastic response of the surfactant/water system.[33] The aqueous Pluronic solution gelled between 40 and 50 wt.-%. Recall that the drop radius measurements (Fig. 1b) showed that the drying process is diffusion limited for $t < 210$ s. In this regime, from mass balance at the free surface, the time required for the concentration to reach the critical value at which crust formation occurs can be estimated by $t_c = D(\varphi_c)(\varphi_c - \varphi_0)^2 S^2/J_o^2$, where φ_0 is the initial volume fraction of the polymer, φ_c is the polymer-volume fraction at the free surface, D is the diffusion coefficient, and S is the surface area.[18] The diffusion coefficient of F68 in aqueous solution at the critical concentration (50 wt.-% ≃ 59 mM) is 2×10^{-6} cm^2 s^{-1}.[34] Using these values and the surface area of the drop when it reaches a fixed base radius gives $t_c = 102$ s. The drying time corresponding to a fixed evaporation rate J_o is $t_d = 540$ s. Similar to the findings of Pauchard and Allain,[19] because $t_c < t_d$, the crust forms before the drying of the drop is complete; evaporation proceeds at a slower rate through a porous mesh-like crust, and loss of volume enclosed leads to the surface undulation.

In summary, we have demonstrated the formation of a thin film (~100 nm) at the free surface of a drying drop of SWNT–F68 on a substrate. Crust formation can be explained qualitatively by de Gennes theory; a quantitative prediction of the thickness of the crust would require a theory that includes polymer adsorption at the free surface. The phenomenon of crusting at the free surface due to solvent mass transfer across an interface may be exploited to fabricate thin crusts and coatings of SWNTs on substrates.

Experimental

The solvent was F68 Pluronic dissolved in water at a concentration of 2 wt.-% or 2.4 mM (critical micelle concentration, 1.4 mM [35]). F68 is a high-molecular-weight ($M_w = 8400$ g mol^{-1}) surfactant with two PEO chains connected by a PPO chain, $PEO_{78}(PPO_{30})$ PEO_{78}, that forms lyotropic cubic phases at high concentrations and/or low temperature [29]. SWNTs (HiPco, Rice University; HPR 120.3) were dispersed in the surfactant solution through a technique developed by O'Connell et al. [36], involving homogenization, ultrasonication, and ultracentrifugation to obtain suspensions with final concentrations between 20 and 30 mg L^{-1}. The hydrophobic segment of the surfactant (PPO) sits at the surface of individual carbon nanotubes (the exact configuration of PPO on the nanotube surface is still unclear), whereas the two hydrophilic PEO segments expand in water. The polymer provides a steric barrier to bundling induced by van der Waals forces between nanotubes; such Pluronic-stabilized suspensions of individual SWNTs were stable for months. The SWNTs in the suspensions were not aggregated: Raman fluorescence spectroscopy showed high-energy fluorescence peaks, and the Raman peak at ~273 cm^{-1}(indicative of bundles [37,38]) was suppressed.

Glass slides were cleaned in a solution of 70 % sulfuric acid and 30 % hydrogen peroxide for 30 min, rinsed in water, and wiped clean with methanol. 1 μL drops of the dispersion were deposited on the substrate and allowed to dry under ambient conditions (23 °C and 38 % relative humidity). Dried-drop samples were investigated using a Zeiss Axioplan-2 optical microscope, a tapping mode Digital Instrument Nanoscope IIIA atomic force microscope, a JEM 2010 transmission electron microscope, and a JEOL 5300 scanning electron microscope. The crust was floated on water and transferred to appropriate

ADVANCED MATERIALS

substrates: onto mica for AFM, onto clean SEM posts, and onto copper grids for TEM. The crusts could be floated on water for over 48 h without resuspension.

Received: March 24, 2005
Final version: August 26, 2005
Published online: November 15, 2005

[1] R. H. Baughman, A. A. Zakhidov, W. A. de Heer, *Science* **2002**, *297*, 787.
[2] B. Vigolo, A. Pénicaud, C. Coulon, C. Sauder, R. Pailler, C. Journet, P. Bernier, P. Poulin, *Science* **2000**, *290*, 1331.
[3] Z. Wu, Z. Chen, L. J. M. Du, X. J. Sippel, M. Nikolou, K. Kamaras, J. R. Reynolds, D. B. Tanner, A. F. Hebard, A. G. Rinzler, *Science* **2004**, *305*, 1273.
[4] X. Zhang, T. V. Sreekumar, T. Liu, S. Kumar, *J. Phys. Chem. B* **2004**, *108*, 16435.
[5] R. Ramasubramaniam, J. Chen, H. Liu, *Appl. Phys. Lett.* **2003**, *83*, 2928.
[6] B. Kim, J. Lee, I. Yo, *J. Appl. Phys.* **2003**, *94*, 6724.
[7] Y. Murakami, S. Chiashi, Y. Miyauchi, M. Hu, M. Ogura, T. Okubo, S. Maruyama, *Chem. Phys. Lett.* **2004**, *385*, 298.
[8] R. Blossey, A. Bosio, *Langmuir* **2002**, *18*, 2952.
[9] F. Fan, K. J. Stebe, *Langmuir* **2004**, *20*, 3062.
[10] C. Annarelli, L. Reyes, J. Fornazero, J. Bert, R. Cohen, A. W. Coleman, *Cryst. Eng.* **1999**, *2*, 79.
[11] S. S. Abramchuk, A. R. Khokhlov, T. Iwataki, H. Oana, K. Yoshikawa, *Europhys. Lett.* **2001**, *55*, 294.
[12] J. P. Jing, J. Reed, J. Huang, X. H. Hu, V. Clarke, J. Edington, D. Housman, T. S. Anantharaman, E. J. Huff, B. Mishra, B. Porter, A. Shenker, E. Wolfson, C. Hiort, R. Kantor, C. Aston, D. C. Schwartz, *Proc. Natl. Acad. Sci. USA* **1998**, *95*, 8046.
[13] H. Shimoda, S. J. Oh, H. Z. Geng, R. J. Walker, X. B. Zhang, L. E. McNeil, O. Zhou, *Adv. Mater.* **2002**, *14*, 899.
[14] K. S. Birdi, D. T. Vu, *J. Adhes. Sci. Technol.* **1993**, *7*, 485.
[15] R. D. Deegan, O. Bakajin, T. F. Dupont, G. Huber, S. R. Nagel, T. A. Witten, *Nature* **1997**, *389*, 827.
[16] R. D. Deegan, *Phys. Rev. E: Stat. Phys., Plasmas, Fluids, Relat. Interdicip. Top.* **2000**, *61*, 475.
[17] R. D. Deegan, O. Bakajin, T. F. Dupont, G. Huber, S. R. Nagel, T. A. Witten, *Phys. Rev. E: Stat. Phys., Plasmas, Fluids, Relat. Interdiscip. Top.* **2000**, *62*, 756.
[18] L. Pauchard, C. Allain, *Phys. Rev. E: Stat., Nonlinear, Soft Matter Phys.* **2003**, *68*, 52801.
[19] L. Pauchard, C. Allain, *C. R. Phys.* **2003**, *4*, 231.
[20] D. Bornside, C. Macosko, L. Scriven, *J. Appl. Phys.* **1989**, *66*, 5185.
[21] E. Cimapi, P. J. McDonald, *Macromolecules* **2003**, *36*, 8398.
[22] P. G. de Gennes, *Eur. Phys. J. E* **2002**, *7*, 31.
[23] K. S. Birdi, D. T. Vu, A. Winter, *J. Phys. Chem.* **1989**, *93*, 3702.
[24] F. Parisse, C. Allain, *Langmuir* **1997**, *13*, 3598.
[25] M. G. Muñoz, F. Monroy, F. Ortega, R. G. Rubio, D. Langevin, *Langmuir* **2000**, *16*, 1083.
[26] M. F. Islam, A. M. Alsayed, Z. Dogic, J. Zhang, T. C. Lubensky, A. G. Yodh, *Phys. Rev. Lett.* **2004**, *92*, 088303.
[27] M. F. Islam, M. Nobili, F. Ye, T. C. Lubensky, A. G. Yodh, *Phys. Rev. Lett.* **2005**, *95*, 148301.
[28] S. T. Hyde, in *Handbook of Applied Surface and Colloid Chemistry* (Ed: K. Holmberg), Wiley, New York **2001**, pp. 299–332.
[29] G. Wanka, H. Hoffmann, W. Ulbricht, *Macromolecules* **1994**, *27*, 4145.
[30] E. Eiser, F. Molino, G. Porte, *Phys. Rev. E: Stat. Phys., Plasmas, Fluids, Relat. Interdiscip. Top.* **2000**, *61*, 6759.
[31] M. J. O'Connell, S. M. Bachilo, C. B. Huffman, V. C. Moore, M. S. Strano, E. H. Haroz, K. L. Rialon, P. J. Boul, W. H. Noon, C. Kittrell, J. P. Ma, R. H. Hauge, R. B. Weisman, R. E. Smalley, *Science* **2002**, *297*, 593.
[32] R. Sedev, D. Exerowa, G. H. Findenegg, *Colloid Polym. Sci.* **2000**, *278*, 119.
[33] See Supporting Information.
[34] M. G. Muñoz, F. Monroy, F. Ortega, R. G. Rubio, D. Langevin, *Langmuir* **2000**, *16*, 1094.
[35] J. R. Lopes, W. Loh, *Langmuir* **1998**, *14*, 750.
[36] M. J. O'Connell, P. Boul, L. M. Ericson, C. Huffman, Y. H. Wang, E. Haroz, C. Kuper, J. Tour, K. D. Ausman, R. E. Smalley, *Chem. Phys. Lett.* **2001**, *342*, 265.
[37] M. S. Strano, V. C. Moore, M. K. Miller, M. J. Allen, E. H. Haroz, C. Kittrell, R. H. Hauge, R. E. Smalley, *J. Nanosci. Nanotechnol.* **2003**, *3*, 81.
[38] V. C. Moore, M. S. Strano, E. H. Haroz, R. H. Hauge, R. E. Smalley, J. Schmidt, Y. Talmon, *Nano Lett.* **2003**, *3*, 1379.

DOI: 10.1002/adma.200501232

Experimental Evidence for Grain-Boundary Sliding in Ultrafine-Grained Aluminum Processed by Severe Plastic Deformation**

By *Nguyen Q. Chinh*,* *Péter Szommer*, *Zenji Horita*, and *Terence G. Langdon*

Processing of metals through the application of severe plastic deformation (SPD) is currently receiving much attention because it has the potential to refine the grain size to submicrometer or nanometer levels.[1] These ultrafine-grained materials have high strength through the Hall–Petch relationship but in practice their utility is generally restricted because they exhibit only limited ductility.[2] There is indirect evidence suggesting that grain-boundary sliding may occur more easily in metals processed by SPD and this may give high strength and a reasonable level of tensile ductility.[2–5] Here we report a direct demonstration of the occurrence of grain-boundary sliding in pure aluminum after SPD processing. Using high purity

[*] Prof. N. Q. Chinh, P. Szommer
Department of General Physics, Eötvös University
Pázmány P. sétány 1/A, 1117 Budapest (Hungary)
E-mail: chinh@metal.elte.hu
Prof. Z. Horita
Department of Materials Science and Engineering
Faculty of Engineering, Kyushu University
Fukuoka 812-8581 (Japan)
Prof. T. G. Langdon
Departments of Aerospace & Mechanical Engineering and Materials Science, University of Southern California
Los Angeles, CA 90089-1453 (USA)

[**] This work was supported in part by the Hungarian National Scientific Research Fund under Contract Numbers OTKA-038048 and 043247 (N. Q. C. and P. S.), in part by the Light Metals Educational Foundation of Japan (Z. H.) and in part by the National Science Foundation of the United States under Grant No. DMR-0243331 (T. G. L.)